GRAPHENE OXIDE AND CARBON NANOTUBE - BASED SATURABLE ABSORBER Q-SWITCHED ERBIUM DOPED FIBER LASER

RAWAN M S SOBOH

FACULTY OF ENGINEERING
UNIVERSITY OF MALAYA
KUALA LUMPUR

2018

GRAPHENE OXIDE AND CARBON NANOTUBE - BASED SATURABLE ABSORBER Q-SWITCHED ERBIUM DOPED FIBER LASER

RAWAN M S SOBOH

DISSERTATION SUBMITTED IN FULFILMENT OF THE REQUIREMENTS FOR THE DEGREE OF MASTER IN ENGINEERING

FACULTY OF ENGINEERING
UNIVERSITY OF MALAYA
KUALA LUMPUR

2018

UNIVERSITY OF MALAYA

ORIGINAL LITERARY WORK DECLARATION

Name of Candidate: Rawan M S Soboh

Matric No: KQH170001

Name of Degree: Master in Engineering (Telecommunication)

Title of Project Paper/Research Report/Dissertation/Thesis ("this Work"):

Graphene Oxide and Carbon Nanotube - Based Saturable Absorber Q-Switched Erbium Doped Fiber Laser

Field of Study: Photonic (Electronic and Automation)

I do solemnly and sincerely declare that:

(1) I am the sole author/writer of this Work;
(2) This Work is original;
(3) Any use of any work in which copyright exists was done by way of fair dealing and for permitted purposes and any excerpt or extract from, or reference to or reproduction of any copyright work has been disclosed expressly and sufficiently and the title of the Work and its authorship have been acknowledged in this Work;
(4) I do not have any actual knowledge nor do I ought reasonably to know that the making of this work constitutes an infringement of any copyright work;
(5) I hereby assign all and every rights in the copyright to this Work to the University of Malaya ("UM"), who henceforth shall be owner of the copyright in this Work and that any reproduction or use in any form or by any means whatsoever is prohibited without the written consent of UM having been first had and obtained;
(6) I am fully aware that if in the course of making this Work I have infringed any copyright whether intentionally or otherwise, I may be subject to legal action or any other action as may be determined by UM.

Candidate's Signature Date:

Subscribed and solemnly declared before,

Witness's Signature Date:

Name:

Designation:

ABSTRACT

To date, various Q-switched Erbium doped fiber lasers (EDFLs) have been demonstrated using various types of nanomaterials based saturable absorber (SA) such as graphene, topological insulators, transition metal dichalcogenides. In this report, Q-switched EDFLs have been demonstrated two types of SAs; graphene oxide (GO) and carbon nanotube (CNT) films. The CNT and GO based SA was successfully fabricated by embedding the nanoparticles into polyethylene oxide (PEO) and polyvinyl alcohol (PVA), respectively. Both films were characterized by FESEM and XRD. The CNT based Q-switched EDFL produces a pulse train operating at 1559.04 nm. The repetition rate of the pulse train is tunable within 31.5 kHz to 55.04kHz as the pump power is varied from 0 mW to 28.38 mW. The maximum pulse energy of 47.7834 nJ and the lowest pulse width of 5 µs were obtained at the pump power of 28.38 mW. The RF spectrum of the pulse train shows signal to noise ratio of about 74 dB, which indicates the stability of the laser. On the other hand, GO based EDFL produces a stable Q-switching pulse operating at 1558.186 nm at threshold pump power of -2.49mW. The repetition rate of the laser varies from 22.32 kHz and 69.83 kHz as the 980-nm pump power increased from -2.49 mW to 28.38 mW. The Q-switching operating has the shortest pulse width of 5 µs, the maximum pulse energy up to 98.73 nJ and the peak-to-pedestal ratio of 70 dB indicating the high stability of the laser. These results indicate that GO film performed better than CNT in terms of lower threshold pump power and better stability. Both SA have a great potential for pulse generation at 1.5 µm.

ABSTRAK

Sehingga kini, pelbagai jenis laser gentian doped Erbium (EDFLs) telah ditunjukkan menggunakan pelbagai jenis bahan penyerap yang berasaskan nanomaterials seperti graphene, penebat topologi, dichalcogenides logam peralihan. Dalam laporan ini, EDFLs Q-switch telah ditunjukkan dua jenis SAs; filem-filem graphene oxide (GO) dan nanotube karbon (CNT). SA berasaskan CNT dan GO telah berjaya direka dengan memasukkan nanopartikel ke dalam polietilen oksida (PEO) dan polyvinyl alcohol (PVA), masing-masing. Kedua-dua filem itu dicirikan oleh FESEM dan XRD. EDFL Q-switch yang berasaskan CNT menghasilkan kereta api denyut beroperasi pada 1559.04 nm. Kadar pengulangan kereta denyut boleh berubah dalam 31.5 kHz ke 55.04kHz kerana kuasa pam berubah dari 0 mW hingga 28.38 mW. Tenaga denyut maksimum 47.7834 nJ dan lebar nadi terendah 5 μ diperolehi pada daya pam 28.38 mW. Spektrum RF kereta nadi menunjukkan isyarat kepada nisbah bunyi kira-kira 74 dB, yang menunjukkan kestabilan laser. Sebaliknya, GO berasaskan EDFL menghasilkan stabil Q-switching beroperasi pada 1558.186 nm pada kuasa pam ambang sebanyak -2.49mW. Kadar pengulangan laser berbeza dari 22.32 kHz dan 69.83 kHz kerana kuasa pam 980-nm meningkat dari -2.49 mW hingga 28.38 mW. Operasi Q-switching mempunyai lebar denyut terpendek 5 μs, tenaga denyut maksimum hingga 98.73 nJ dan nisbah puncak-ke-alas 70 dB menunjukkan kestabilan tinggi laser. Keputusan ini menunjukkan bahawa filem GO lebih baik daripada CNT dari segi kuasa pam ambang yang lebih rendah dan kestabilan yang lebih baik. Kedua-dua SA mempunyai potensi besar untuk penjanaan nadi pada 1.5 μm.

.

ACKNOWLEDGEMENTS

First and foremost, all praise is due to Allah, the most compassionate and the most merciful, who enables me and give me the strength and health to do this work, then all the praise to the holy prophet Muhammad (peace be upon him), the city of knowledge.

Secondly, To the fountain of patience and optimism and hope to each of the following in the presence of God and His Messenger, my mother dear. To those who have demonstrated to me what is the most beautiful of my husband & son life. To the big heart my dear father. To the people who paved our way of science and knowledge All our teachers distinguished. To the taste of the most beautiful moments with my friends.

Thirdly, I offer my sincerest gratitude to my supervisor, Prof. Ir. Dr. Sulaiman Wadi Harun, who has supported me throughout my research project with his patience and knowledge whilst allowing me the room to work in my own way. One simply could not wish for a better or friendlier supervisor.

My sincere thanks also go to Dr. Mahmoud Hazzaa, Mohammed Ahmed, Dr. Farhana and Dr. Faisal.

Special mention goes to my husband FUAD for the infinity support, motivate and care along the way of my master degree, which is only the tip of the iceberg.

Finally, many thanks should go to whoever contributed, directly or indirectly, in producing the final form of the present work, especially my friends.

TABLE OF CONTENTS

LIST OF FIGURES

LIST OF TABLES

LIST OF SYMBOLS AND ABBREVIATIONS

BP	:	Black phosphorus
Be_2Se_3	:	Bismuth selenide
CNT	:	Carbon Nanotubes
CW	:	Continuous wave
dB	:	Decibel
dB/m	:	Decibel/meter
Ec	:	Conductance band
EDFL	:	Erbium doped fiber laser
Eg	:	Bandgap Energy
Er^{3+}	:	Erbium
Ev	:	Valence band
FESEM	:	Field emission scanning electron microscope
Fig	:	Figure
GO	:	Graphene Oxide
GVD	:	Group velocity dispersion
Ho	:	Holmium
Hv	:	Photon energy
KHz	:	Kilo Hertz
M	:	Metal
MHz	:	Mega Hertz
MoS_2	:	Molybdenum disulphide
mW	:	Miliwatts
NA	:	Numerical aperture
Nd^{3+}	:	Neodymium

NiO	:	Nickel oxide
nJ	:	Nanojoule
NPR	:	Nonlinear polarization rotation
OSA	:	Optical spectrum analyzer
OSC	:	Oscilloscope
PEO	:	Poly ethylene oxide
Pr^{3+}	:	Praseodymium
Ps	:	Picoseconds
RF	:	Radio frequency
SA	:	Saturable absorber
Sec	:	Second
SESAM	:	Semiconductor saturable absorber mirror
SMF	:	Single mode fiber
SNR	:	Signal-to-noise ratio
SWCNT	:	Single-walled carbon nanotubes
TBP	:	Time bandwidth product
TI	:	Topological insulator
TMD	:	Transition-metal dichalcogenides
WDM	:	Wavelength division multiplexer
WS^2	:	Tungsten disulphide
XRD	:	X-ray diffraction
Yb	:	Ytterbium
YDFL	:	Ytterbium-doped fiber laser
ZnO	:	Zinc oxide
μm	:	micrometer

CHAPTER 1: INTRODUCTION

1.1 Research Motivation

There are many advantages of fiber laser that we can get, for example high power, high stability, and high reliability so that make it the focus of attention and interest, as a result the optical fiber technology become progressively more advanced and higher quality. Very recently, laser based on rare-earth doped fiber has attracted a lot of attentions that simulates an evolution on the technique of fiber fabrication. At 60's, the use of optical fiber to reduce the pump power for demonstrate the gain in glass lasers. at a wavelength of around 1 µm, the first rare-earth-doped fiber lasers have fabricated a few milliwatts (Maiman, 1960). As seen in figure 1.1, a huge revolution of fiber lasers has been occurred when it enters the region of powers in kilowatt. The coupling of the pump light inside the fiber can achieve when the diode-pumped lasers and double-clad fibers are reliable and high-brightness.

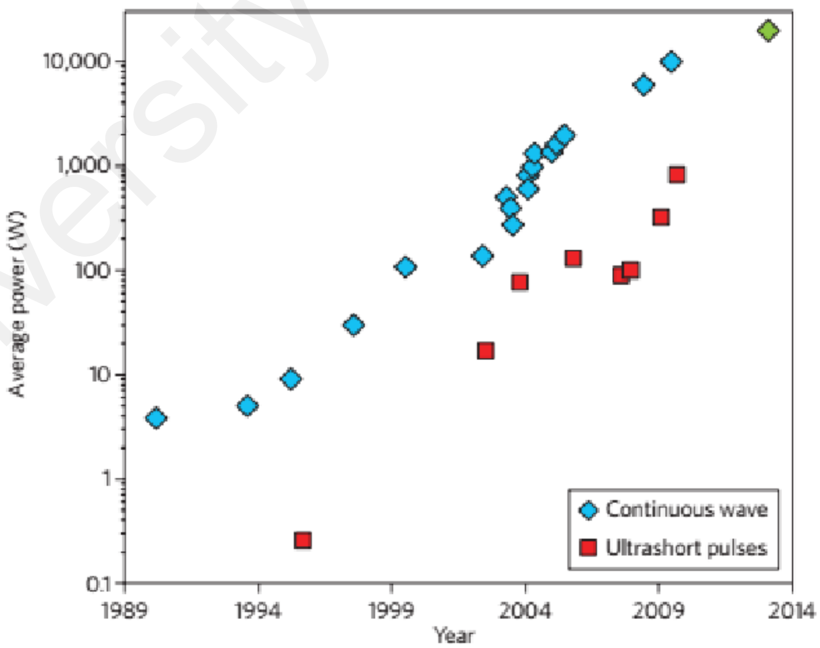

Figure 1.1: The growth of fiber laser over the past 25 years (Jauregui, Limpert, & Tünnermann, 2013)

The fiber doped use many ingredients of rare-earth for gain medium like Neodymium, Ytterbium, Holmium, Thulium, Erbium, and Praseodymium. Nevertheless, Ytterbium (Yb3+) and Erbium (Er3+) have pervaded the industry of fiber lasers. The wavelength of operation for Erbium-doped fiber laser (EDFL) is between 1520 and to 1560 nm, that is stead for fiber communication however the operation wavelength for Ytterbium-doped fiber laser (YDFL) is between 1030 nm and 1100 nm, that is repeatedly used for high power. This work talks about EDFL, which has the most elevated demand because it has many benefits like small size, great beam quality, low cost and broad tunable wavelength. (J. Wang, Yang, Wei, & Zhou, 2015)

The supreme demand in manufacturing and medication in application of communication is ultra-short pulse laser. undeniably that this demand is very high because it can supply a very fine, high and fast resolution micro-processing that as a result of high repetition rate. The pulsed laser is created by a rife technique which is a Q-switch. The Q-switch is adjusting the quality factor Q of the laser cavity to create a train of pluses, which is quite short and intense pulses with a higher Q factor. So that, it is lead to low loses for each oscillation cycle. The ratio of energy presents the Q-factor, which is kept in the active medium. This energy is used to empower the loses per oscillation cycle.

Fiber lasers which is passively Q-switched can obtain a mass of applications in the medicine, material processing, communications and manufacturing, moreover basic research and what have because of their soft design, that allows for the development of built-in and cost-effective pulsed laser sources (Fermann & Hartl, 2013). Although active components can operate Q-switch, saturable absorbers (SAs) can provide a great advantage of ease of operation. actively Q-switch, needed additional equipment like acoustic or electro-optic and modulator that require complicated circuit to produce pulse (Pérez-Millán, Cruz, & Andrés, 2005), thus generate the pulsed laser system need more cost and work (Harith Ahmad et al., 2014). So, passive method was introduced by discovery of saturable absorber is introducing passive method. That to solve the problem confronting active method.

An ideal SA Is characterized by a broadband absorption, ultrafast recovery time (~ps), less saturation strength, proper modulation depth, critical damage threshold and efficient-time as well as cost to create. SAs has two types, artificial SAs and real passively Q-switch is achieved by SAs. Figure 1.2 shows the timeline discovery of real SAs since 1964. using nonlinear polarization rotation (NPR) is used to make SAs (Luo et al., 2011), semiconductor saturable absorber mirrors (SESAMs) (D. R. R. P. E. S. A. Paschotta), and single-walled carbon nanotubes (SWCNT) (Jiang et al., 2016). However, SAs has many drawbacks like complex process of fabrication, complicated optical alignments, high sensitivity to surrounding, narrow operating bandwidth and limit the function of these SAs (Li et al., 2015). Still, ultrafast carrier dynamics and ultra-broadband absorption are made the graphene one of the most demanded as a saturable absorber. The invention of new 2D materials like topological insulators (TIs), transition-metal dichalcogenides (TMDs) and black phosphorus (BP) thanks to the success of graphene in photonic implementations. Recently, TIs materials like bismuth selenide (Be2Se3) (H Ahmad et al., 2015) and TMDs materials like tungsten disulphide (WS2) (H Ahmad, NE Ruslan, MA Ismail, SA Reduan, et al., 2016), and molybdenum disulphide (MoS2) (Harith Ahmad et al., 2016). In addition to black phosphorus-based SA (E. Ismail, A. Kadir, A. Latiff, H. Ahmad, & S. Harun, 2016) have been investigated and broadly reported as they are having the same performance as graphene. zinc oxide (ZnO) nanoparticles considers as a transition metal oxides (H Ahmad, CSJ Lee, et al., 2016) and iron oxide (Fe304) (Bai et al., 2016) are also attracted many interests in recent years for pulse laser generation. These materials are also belonging to nanomaterials category.

1.2 Objective

The goals of this research are to explain the usage of graphene oxide (GO) and carbon nanotube (CNT) as saturable absorber with a Q-switched fiber laser. This research work is guided by the following objectives:

i. To fabricate and characterize transition metal oxides-based SA.

ii. To demonstrate Q-switching pulse generation using the SA.

1.3 Research Overview

This research report consists of 5 chapters, which carefully demonstrate pulsed fiber lasers operation using two different nanomaterials-based SA; graphene oxide (GO) and carbon nanotube (CNT). This first chapter introduces the topic, where motivation of this study as well as the research objectives, are also briefly described.

In chapter 2, a literature study on erbium doped fiber laser and saturable absorption principle are described. This chapter also describes the saturable absorption process that leads to the generation of Q-switched pulse laser also the important parameter to estimate the performances of the Q-switched fiber laser.

Chapter 3 demonstrates the fabrication and characterization of two types of transition metal oxides saturable absorbers; GO and CNT. The characterization data from FESEM. Graphene oxide (GO) nanoparticles are embedded in PVA film to act as a SA. CNT nanoparticles are embedded in PEO film to act as a SA. The metal oxide film is sandwiched between fiber ferrule and incorporated in a ring-cavity Q-switched erbium doped fiber laser (EDFL) cavity for pulse train generation.

Chapter 4 presents the results for both experiments. The results obtained indicates that both GO and CNT nanoparticles give good response for a SA in passively Q-switched fiber laser operating at a low pump strength.

Chapter 5 concludes the finding of the research and proposes a recommendation for further work

CHAPTER 2: LITERATURE REVIEW

2.1 Erbium-doped Fiber Laser

An erbium-doped fiber (EDF) is an optical fiber of which the core is doped with rare-earth element erbium ions, Er3+. The main reasons rare earth elements are used in the optical fiber is because of the glass consists of rare earth ions are optically active. Which mean, they can absorb the light at one wavelength and release the coherent light at different wavelength. Erbium-doped fiber lasers (EDFLs) are fiber lasers with an EDF as the gain medium and they are used as sources for coherent light signal generation operating at 1550 nm region. All EDFLs can be pumped with efficient, cheap laser diodes, and compact operating at 980 nm or 1480 nm. The negligible coupling losses is the main feature of EDFL because of the compatibility with various fibers and fiber optic components used in communications. This behavior is very useful for creating a laser, coherent broadband sources or to amplify the signal at the emission wavelength of 1550 nm (Méndez & Morse, 2011). Table 2.1 shows the rare earth ions and its host glasses and also their emission wavelength ranges. Some example of rare earth ions that use in fiber doped gain medium such as Ytterbium (Yb3+), Holmium (Ho3+), Erbium (Er3+), Neodymium (Nd3+), Thulium (Tm3+), and Praseodymium (Pr3+).

Table 2.1: Rare earth ions with their common host glasses and emission wavelength

Ion	Erbium (Er^{3+})	Praseodymium (Pr^{3+})	Neodymium (Nd^{3+})	Thulium (Tm^{3+})	Ytterbium (Yb^{3+})	Holmium (Ho^{3+})
Common Host Glasses	Silicate, Phosphate and Fluoride Glasses	Silicate and Fluoride Glasses	Silicate and Fluoride Glasses	Silicate, germanate and Fluoride Glasses	Silicate Glass	Silicate and Fluorozir Conate Glasses
Emission Wavelength (µm)	1.5-1.6, 2.7, 0.55	1.3, 0.635, 0.6, 0.52, 0.49	1.03-1.1, 0.9-0.95, 1.32-1.35	1.7-2.1, 1.45-1.53, 0.48, 0.8	1.0-1.1	2.1, 2.9

EDFLs also have been studied in a broad of scope as a source in a communication system that operates in the 3rd communication window in the range from 1.5 to 1.62 µm.

EDFLs can generate continuous wave and pulses sources with a broadband and narrowband on the 4 I13/24 I15/2 transition of erbium. Figure 2.1 indicates the energy level in silica fibers of Erbium ions (Er3+). The principal absorption bands of Er3+ ions is at ~980 nm and at 1480 nm which are suitable for the optical pumping (Okhotnikov, Kuzmin, & Salcedo, 1994). By pumping the EDF with 980 nm pump, the Erbium ions absorbs the pump photons so that it is excited to 4 I11/2 before fast decaying to 4 I13/2. The continuous pumping creates a population inversion between 4 I11/2 and the ground state, which then emits spontaneous and stimulated photons in 1550 nm region. In a laser cavity, the amplified spontaneous light (ASE) oscillates and generates laser.

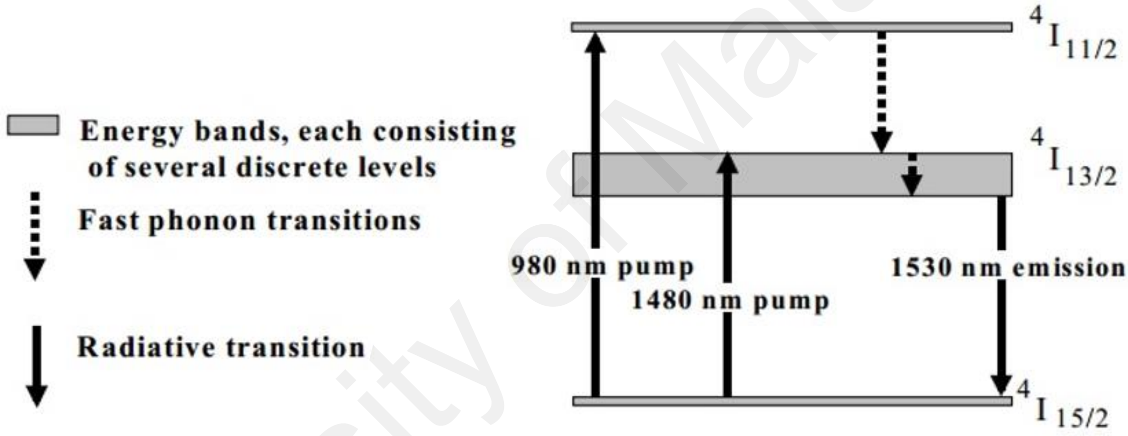

Figure 2.1: Energy diagram of Erbium (Er^{3+}) in silica fibers (Citation)

The key features of EDF is its spectrum is broad ranging and the fiber dispersion at 1.5 µm is irregular, therefore the EDF has advantageous for ultra-fast and ultra-short fiber lasers. The irregular dispersion and nonlinearity in the soliton pulse regime of the fiber laser are self-adjusting pulse that is flexible to noise and loss and also stable. This gives advantage in a long-distance and high-speed bandwidth of optical fiber communications.

2.2 Saturable Absorber

A saturable absorber (SA) is a nonlinear optical material with a certain optical loss, which is decreased at high optical intensities. A saturable absorber has very unique optical properties such as ultrafast recovery time (~ps),a broadband absorption, high modulation depth, and low saturation intensity that make them useful for several lasers (fiber, solid state, semiconductor) operating at various wavelengths range from 500 to 2500 nm (Sobon, 2016). Two sorts of saturable absorbers are presented: real SAs and artificial SAs. When the intrinsic nonlinear absorption of materials is decrease with the increasing of light intensity, the material is classified as real SA. For devices that manipulate nonlinear effects to imitate the action of a real SA by causing an intensity dependent transmission, is classified as artificial SA. In this research study, real SAs are only considered. The ideal features of SA are efficient time and cost as well as high damage threshold. The purposes of SAs are for the generation of ultrashort pulses in passive Q-switched fiber laser. Outside laser resonators for nonlinear filtering is one usage of saturable absorbers, for example used in optical signal processing and to clean up pulse shapes (D. R. R. P. E. S. A. Paschotta). A saturable absorber for Q switching consists of a material that absorbs at the laser wavelength and has a small amount of saturation intensity. A saturable absorber should have the characteristics as stated below:

- For the maximum pulse energy, the modulation depth (maximum loss reduction) should be approximately equal to one and a half of the initial gain and non-saturable losses should be as lower as possible. While, for lower pulse energy and higher repetition rate, a smaller depth is suitable.
- The saturation energy of the gain medium must be lower to ensure that the fast saturation of the absorber can be kept and the loss 9 of pulse energy is kept to minimum level.
- The recovery time of the absorber must be longer than the pulse duration but the time is sufficient to ensure that the loss is recovered before the gain after the emission of the pulse.

Fig. 2.2 describes the working principle of the SA. Fig. 2.2 (a) illustrates the principle of saturable absorption process. In this process, the light will be absorbed by SAs when the photon energy (hv) is higher than SA bandgap energy, Eg to excite carriers from the valence band, Ev to the conduction band, Ec which will produce electron-hole pairs. By referring to Pauli Exclusion Principle, when the excited state of the SA is fully occupied with the excited carriers, the SA tends to be in saturation mode, where there is no more photon can be absorbed. At this instant, SA will become transparent; this can be shown as in Fig. 2.2 (b). When this occurred, additional photons that pass through will induce electron-hole recombination and excited state absorption. This will lead to massive photon release, which will generate a sudden intense light, and the carriers will fall back to the ground state. Then, the transmitted light intensity will have reduced and the SA will recover its saturable absorption again. Normally, low intensity of light will be absorbed by the absorber and high intensity of light will pass through the absorber and generated the pulses.

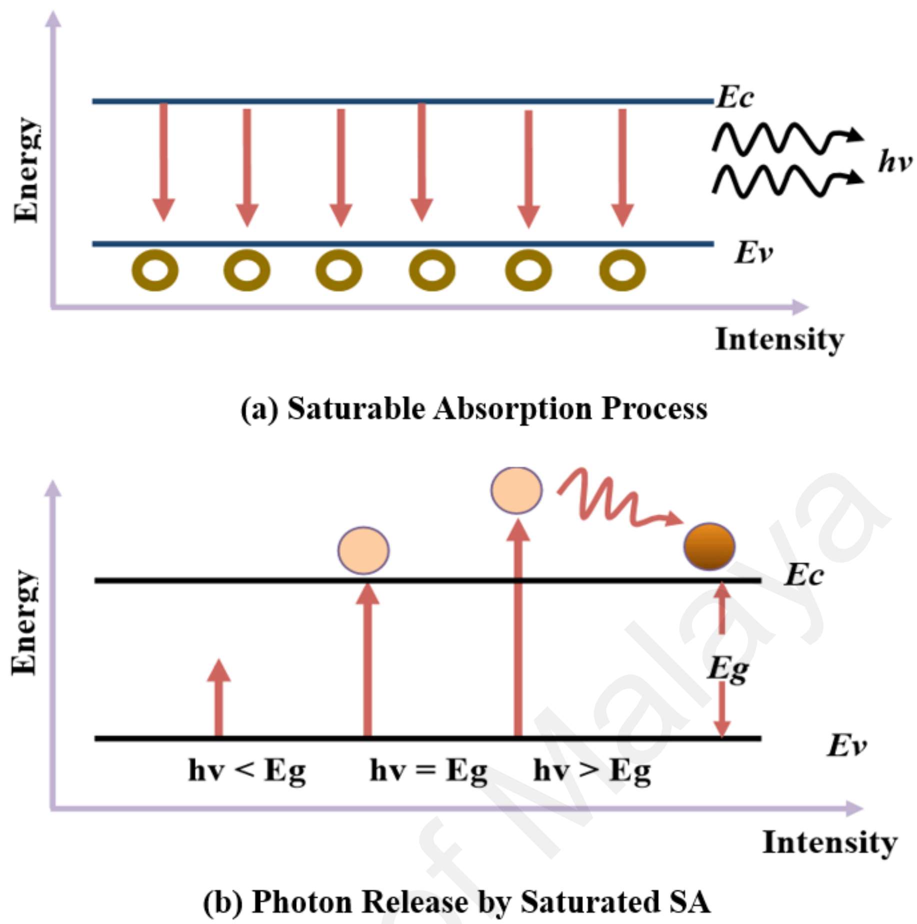

Figure 2.2: Working principle of SA (a) saturable absorption process and (b) light emission by the saturated SA

2.3 Q-Switching

It is a technique to generate a pulse laser. This technique will generate a pulse of light with a very high peak power (~ gigawatt), which is much higher than the power produced in continuous wave (cw) mode. Q-switching will produce low repetition rate pulse, high pulse energy, and broader pulse durations, compared to the mode locking technique. In Q-switching technique, we are able to achieve a single solid and short pulse trains of laser radiation (Singh, Zeng, Guo, & Cai, 2012). The primary methods of Q-switching are passive Q-switching and active Q-switching.

Normally, active Q-switching requires electrically powered equipment such as electro-optics and acoustic-optics modulators. This modulator will add more cost and complexity as well as produce high loss in the cavity (H Ahmad, NE Ruslan, MA Ismail, ZA Ali, et al., 2016). Passive Q-switching technique can be achieved through the employment of SA as the Q-switcher.

In the telecommunication area, range finding, material processing, and medicine, the train of Q-switching pulses are applicable and generated by Passive Q-switch fiber lasers. In the presence of different gain media, the high energy per pulse and a wide tuning range are the benefits of using the Q-switch technique as compared to mode-locked fiber lasers. Generally, passive lasers are relatively low cost, provide stable, simple in design, as well as consistent output power. Fig. 2.3 illustrates the basic structure of the passive Q-switched laser cavity (Rüdiger Paschotta, 2008).

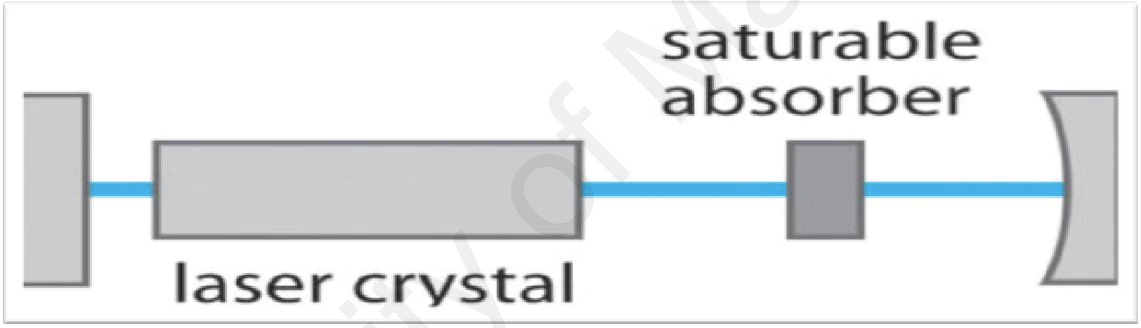

Figure 2.3: Basic structure of passive Q-switch device

For passive Q switching, the saturable absorbers are automatically modulated the losses as shown in Fig. 2.4. The operation of the pulse generation in passive Q-switched laser is different from the process that running in the active Q-switched laser where in the early process, the losses is introduced by the Q-switched are too high for laser process to start. However, the lasing action begins at a low power level and start to grow at a low rate once the laser gain becomes slightly larger than the total losses. Ideally, the generated laser light can quickly saturate the absorption well before it 12 affects the gain when the saturation energy of the absorber is quite less than the saturation energy of the medium gain which means that the losses is suddenly drop and the net gain (gain – losses ≅ the reduction of the loss by absorber saturation) and therefore the optical power then increases much more rapidly (Rüdiger Paschotta, 2008).

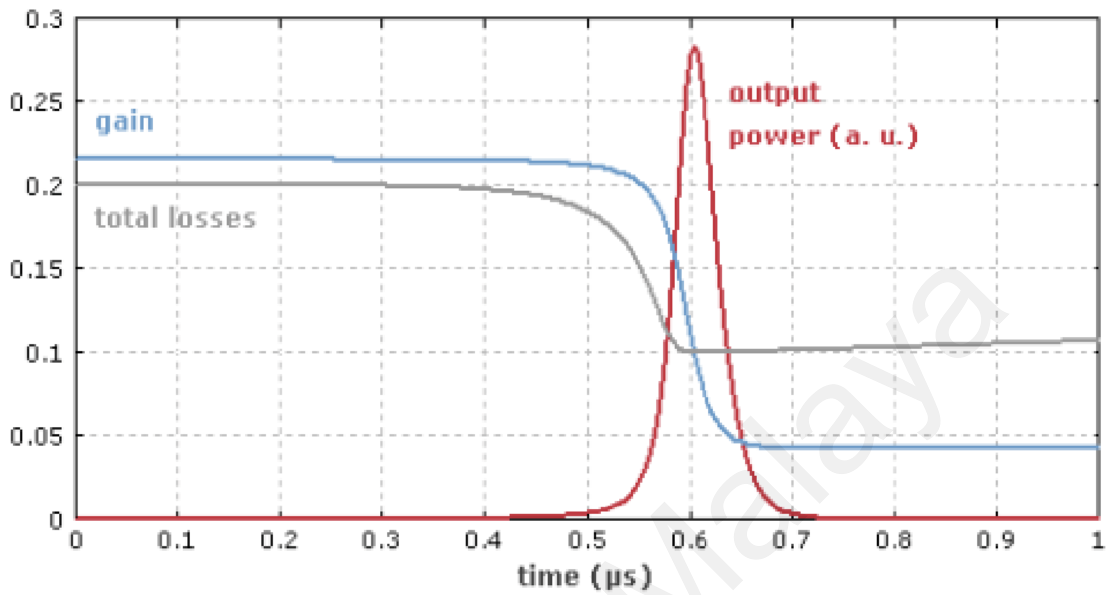

Figure 2.4: Evolution of gain and losses in a passive Q-switching laser

In principle, inside the laser's optical resonator various types of variable attenuator are inserted to generate Q-switch. The operation of the attenuator, the gain medium extracts the light which is not enough to oscillate and making laser light start. The optical resonator quality (Q) factor is decreased because it is corresponded to the attenuation into the cavity. Low resonator losses mean high quality factor per round trip, and vice versa as presented in Figure. 2.5. Q-switcher called a variable attenuator.

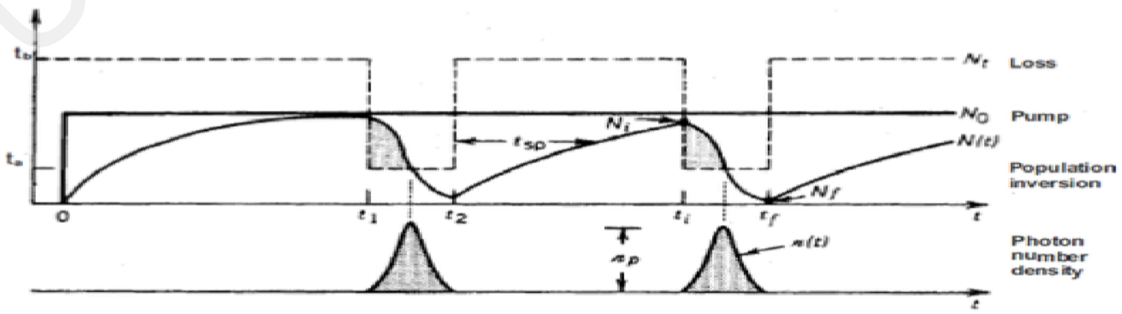

Figure 2.5: Principle of a Q-swithced laser

2.4 Optical Measurements of Fiber Laser

In this research, we have used different equipment to measure the parameters of fiber laser. An oscilloscope with photo-detector are used to measure pulse width and the repetition rate, the wavelength spectrum is analyzing by the optical spectrum analyzer, the input and output power is measured by power meter, and autocorrelator is used to measure the full width at half maximum (FWHM). A few important parameters are used to characterize and evaluates the performances of a pulsed laser such as peak power, repetition rate, pulse duration and pulse energy. Figure 2.6 shows the important parameters in pulsed laser.

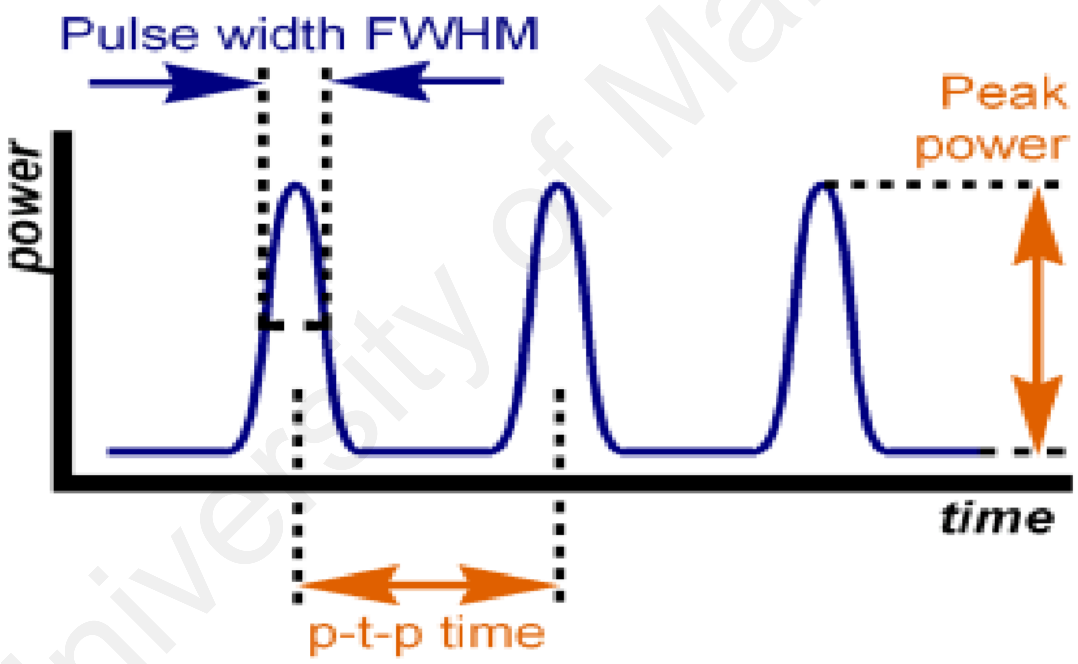

Figure 2.6: Pulse characteristic

2.4.1 Repetition Rate (Rr)

The number of pulses extracts per second (the inverse temporal pulse shaping shape) defined as repetition rate (Rr). The pulse width is inversely proportional to the repetition rate. For Q-switching, the repetition rate varied with the changes of the pump power.

2.4.2 Pulse Width or Pulse Duration (Δt)

The pulse width is defined as the width of the pulse at the half peak power or also known as full width at half maximum (FWHM). Sech2 function or Gaussian function fitting is used in the autocorrelation of the pulse to describe the pulse shape. For the Q-switching, the pulse width is in between nanoseconds regime (Choudhary, Dhingra, D'Urso, Kannan, & Shepherd, 2015).

2.4.3 Pulse Energy (PE)

Pulse energy P_E is the total optical energy content of the pulse. The pulse energy is calculated by dividing the average output power P_O (measured with power meter) by the repetition rate Rr (measured with oscilloscope).

$$P_E = \frac{P_o}{R_r} \tag{2.1}$$

Typical pulse energy for Q-switched laser range from microjoules to millijoules. The pulse energy together with the pulse duration are used to calculate the peak power of the laser pulse.

2.4.4 Peak Power

Peak power P_p is the maximum optical power of the pulse. Due to the short pulse duration, which is possible for optical pulse, the peak power can become very high even for moderately energetic pulse. The FWHM pulse duration (Δt) is used to calculate the peak power, which an optical autocorrelator can measure it and the pulse energy (P_E):

$$P_E = f_s \frac{P_E}{\Delta t} \tag{2.2}$$

where f_s is the numerical factor. The numerical factor depends on the shape of the pulse. For example, Gaussian-shaped pulses using the factor of ~ 0.94 while f_s equals to 0.88 is used for sech2 -shaped pulse. Peak power can be calculated once the pulse shape is known.

2.4.5 Laser efficiency

Slope efficiency, differential efficiency or laser efficiency are known as an optically pumped laser important property. It is defined as the slope of the curve achieved by plotting the laser output power against the pump power. To achieve an optimum efficiency of laser output power of the pump power is usually needs a compromise between the lower threshold pump power and the higher slope efficiency. Laser efficiency is a pump power is converted into laser output power.

$$\eta = \frac{P_{out}}{P_{pump}} \qquad (2.3)$$

where, P_{out} is the laser output power and P_{pump} is the laser pump power of.

2.4.6 Spectral Width (FWHM)

The full width at half maximum (FWHM) is used as a typical method of specifying spectral width. FWHM can be determined in three terms such as in terms of optical frequency (measured in Hz), wavelength (nm), or angular optical frequency (rad/s). The following formula is u sed to convert the small wavelength interval to the frequency bandwidth interval.

$$\Delta v = \Delta\lambda \left(\frac{c}{\lambda^2}\right) \qquad (2.4)$$

CHAPTER 3: SATURABLE ABSORBER PREPARATION AND ALL-FIBER PASSIVELY Q-SWITCHING FIBER LASER SETUP

3.1 Introduction

Recently, Q-switched fiber lasers have obtained a growing interest due to their potential implementations in various areas, for example; micromachining, optical fiber telecommunications and sensing, medicine (R Paschotta et al., 1999), (Siniaeva et al., 2009). In addition, generation fiber lasers have excellent beam quality with high peak power by adjusting the intra-cavity or Q-factor. Q-switch is better than mode-locking laser because of low cost, efficient, and implementation is easy. Mode-locking laser requires a critical prototype of the cavity due to balancing the nonlinearity parameters and dispersion (Marowsky, 1976). The saturable absorbers in a passive Q-switched has several advantages such as compactness, simplicity, and flexibility of applications compared to active mode (Popa et al., 2011). Carbon nanotubes (Anyi, Ali, Rahman, Harun, & Arof, 2013) and graphene (M. Ismail, Ahmad, Harun, Arof, & Ahmad, 2013) are commonly used as SA for passively Q-switched erbium-doped fiber lasers (EDFLs). Carbon nanotubes have been considered as excellent SA as it can be easily fabricated with low cost. However, the chirality and nanotube diameters are determining the operation wavelength by (Kasim et al., 2014). One example zero-bandgap material saturable absorption with wavelength-independent is Graphene, which consider as wideband SA. However, 2.3% is a percent of absorption for graphene at 1550 nm region (Martinez, Fuse, & Yamashita, 2011). The carbon nanotube (CNTs) as a` SA were also extensively studied in recent years for generating Q-switched pulse in fiber laser (Hisamuddin et al., 2016; E. Ismail, N. Kadir, A. Latiff, H. Ahmad, & S. Harun, 2016). For instance, molybdenum disulfide (MoS_2) based Q-switched lasers is demonstrated due to their thickness dependent band-gap and unique absorption property (Woodward et al., 2014). However, its fabrication process is complicated.

Likewise, other nanomaterials such as graphene oxide (GO) (H Ahmad, Siti Aisyah Reduan, et al., 2016) was also reported as SA, where they are functioning as good as the conventional material. This material is referred to graphene metal oxide. In this work, the feasibility of Q-switching operation with 2 others typical (TMOs); Graphene oxide and Carbon nanotube is demonstrated. In this chapter, the TMOs- saturable absorbers are fabricated and characterized. Lastly, with these saturable absorbers, a ring-cavity Q-switched erbium-doped fiber laser (EDFL) is constructed.

3.2 Preparation and Characterization of GO and CNT nanoparticles-based SA

3.2.1 Optical deposition technique

In optical deposition technique, the CNT/graphene particle is attracted onto the ferrule tip (Kashiwagi & Yamashita, 2009; Kashiwagi, Yamashita, & Set, 2009; Martinez, Fuse, Xu, & Yamashita, 2010; Nicholson, Windeler, & DiGiovanni, 2007) by injection the intense light into a CNT-graphene-dispersed solution from a fiber-optic end. Relying on the (weak) absorption two types of general effect; thermal effects and the optical gradient force, which leads in the fluid suspension a self-channeling of light. The weak optical gradient force as a result of when the size of particle is smaller than the wavelength. The scattered light direction is random when the density of particle is high and the multiple scattering dominates. The particles are pushed to the beam center because of these effects. Through the quite narrow beam, the self-trap is hard because its requires high particles densities, in turn, there is a effective loss due to multiple scattering. The thermal effect changes the refractive index significantly, but inside liquid when the temperature increases the refractive index decreases (Lamhot, Barak, Peleg, & Segev, 2010).

Thermophoresis is a thermal mechanism in colloidal suspension often observes, which monitors the reaction of temperature gradients on the suspended particles. Besides that, describing the effect of drifting along a temperature gradient on the ability of a macromolecule or particle (Lamhot et al., 2010). Distinguish methods are proposed to deposit the carbon-based saturable absorber to the fiber core, (Nicholson et al., 2007) the most responsible process to make a carbon-based saturable absorber is a thermophoresis via optical deposition. In the solution, when the laser starts with fiber, at the tips a strange convection is observed current centered. The induced current proceeds the carbon-based motes upward toward the fiber end.

The optical deposition is used to prepare the carbon-based saturable absorber, the first step using ultra-sonification process to disperse the carbon-nanotube/graphene bundles. to separate the agglomerated carbon and the macroscopic flakes nanotube/graphene the centrifugation is followed. For optical deposition process (Martinez et al., 2010), only the homogeneous portion is taken. Precise optical power is important when the carbon-based particles deposited to the fiber core. Deposition the carbon-based particles to concentrate it to the area around the fiber core higher optical power is needed, while adhere the CNT to the fiber core low power is required. 1 dB if the difference between the optimal and higher optical power (Ji et al., 2008). Many factors affected the optimum optical power, for example, solution temperature, the size of particles, concentration scales of the solution, and the optical wavelength used in the deposition process (Ji et al., 2008; Nicholson et al., 2007). To monitor the process of optical deposition, [50] has inventive a setup that needs optical circulator and power meters. For controlling the insertion loss, the duration of the deposition has to be observed. Higher enrolment loss is affected by Long deposition duration.

A little amount of carbon nanotube/graphene is required as saturable absorber in optical deposition technique. However, the big scattering loss is the disadvantages of this technique (Shinji Yamashita, 2012), and the required optical power is easy to influence by many factors to make the carbon nanotube/graphene particles abide to the fiber core.

Furthermore, 1 dB if the difference between the optimal and higher optical power, so the success margin is small.

3.2.2 Drop cast technique

Drop cast technique is modest and straightforward. Trickle a graphene/SWCNT solution onto a fiber ferrule and allow it dry to produce a SA. The SA enrolment loss can be barred relying on the concentration of the solution and the grist of times this process is refined. The process can also be refined until the coveted insertion loss is completed. Though the insertion loss is high, that can be beat by increasing the pulse energy. As the pulse energy rely on the power and frequency, it can be modified by increasing pump power and/or lengthen the fiber laser cavity. The obstacles of this technique are which in the course of increasing the pulse energy, we change the repetition rate and pulse width and Scattering loss.

3.2.3 Mechanical exfoliation technique

Mechanical exfoliation employs scotch tape to frequently husk the graphene layers from a Highly Ordered Pyrolitic Graphite (HOPG) or graphitic flakes and carrying the layers to the 50 Fiber Laser face of the fiber interior. A fiberscope is normally used to test that the graphene is transferred immediately onto the core of the fiber ferrule. Mechanically exfoliated graphene SA has been explained by (Chang, Kim, Lee, & Song, 2010, 2011; M. A. Ismail, Harun, Ahmad, & Paul, 2016; Martinez et al., 2011). The feature of this technique is that it harvests the best quality graphene SA. However, the obstacle of this technicality is that it is time-consume-ing. In addition, it might be difficult to monitoring the desired graphene layer(s) that want to be relocate onto the core of the fiber ferrule.

3.2.4 Thin film and polymer composite

SWCNT and graphene thin films have been mentioned in many literatures (Bao et al., 2009; Set et al., 2003; Shinji Yamashita, Set, Goh, & Kikuchi, 2007). For example, (S

Yamashita et al., 2004) splash a liquid with sparse CNTs onto a fiber end face that work as a substrate, when (Set et al., 2003) sandwiched a thin layer of clarified SWCNTs between quartz substrates. CNTs and graphene polymer complex have also been explained in many publications (Hasan et al., 2009; Kelleher et al., 2009; Popa et al., 2011; Sun et al., 2010; F. Wang et al., 2012). multiple types of polymer materials can be used as a steward to graphene and CNTs, such as., polymethylmethacrylate (PMMA), polyamide, and polycarbonate.

The prime advantages of utilizing polymer composite as a steward are that it minimizes scattering and facilitates similar dispersion of CNTs and graphene. It is thin sufficient to be sandwiched between fiber interior and has higher damage threshold parallel to pure CNT/graphene layer. In spite of this, in terms of the amount applied, it is less active than optical deposition technique and involves additional processing. Other kinds of SA are also available, inclusive tapered fiber (Kashiwagi & Yamashita, 2009; Song, Yamashita, Goh, & Set, 2007), D-shaped fiber (Song et al., 2007), add to CNT/graphene solutions rooted in photonic crystal fiber (Lin, Yang, Liou, Yu, & Lin, 2013; Zhao et al., 2013).

3.3 Laser Configuration

The presented passive Q-switch EDFL prototype is shown in Figure 3.1. The long of Erbium-doped fiber (EDF) is 3.3 m (Iso-Gain I-25(980/125), Fiber core; cut-off absorption 35–45; wavelength, 900–970; numerical aperture, 0.23–0.26@ 1550 nm) was used. The 974 nm laser diode (LD) is used to pump the gain medium, wavelength division multiplexer (WDM) is coupled via 980/1550-nm. The fiber-compatible SA is formed by sandwiched fabricated GO or CNT polymer between fiber connecters using a fiber adapter. After that, the fiber-compatible SA integrated inside the laser cavity to operate the Q-switching. To achieve the unidirectional light operation by using isolator. Into the cavity spliced an 80/20 fiber coupler after the isolator. 50/50 fiber coupler used for further divided 20% output port to enable two simultaneous measurements. The rest of the fibers used as standard single mode fiber (SMF-28). a 1.2-GHz photo-detector is combined with A 350-MHz oscilloscope; an optical power meter, radio frequency spectrum analyzer, and an optical spectrum analyzer (YOKOGAWA AQ6370C) were used simultaneously to monitor radio-frequency (RF) spectrum, the spectrum, time profile of the output pulse train, and output power, respectively.

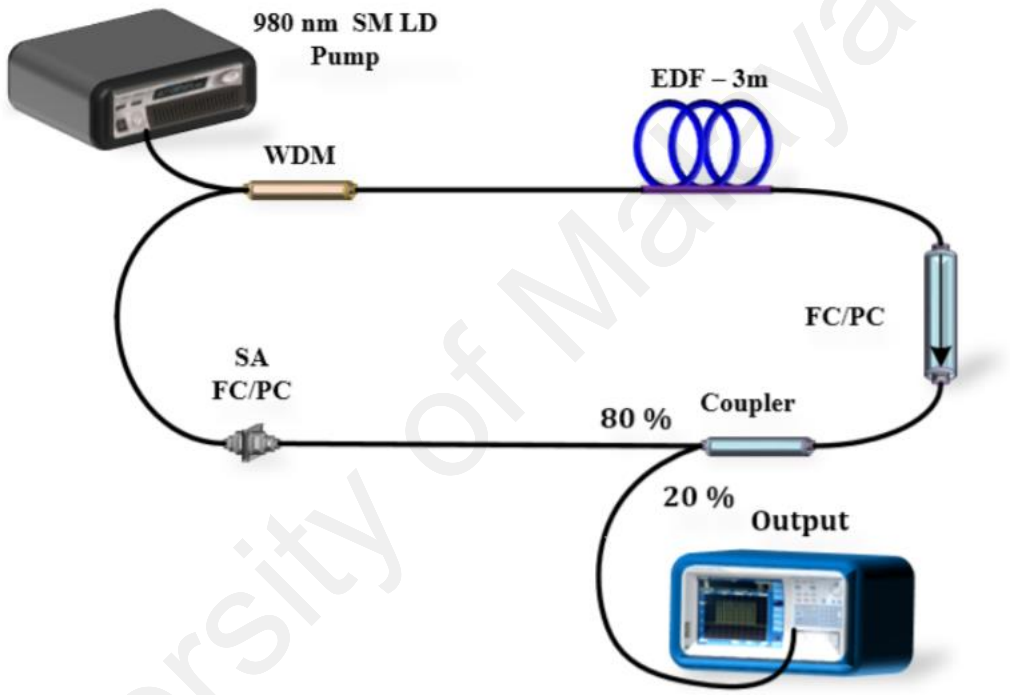

Figure 3.1: Experimental setup of the proposed Q-switched EDFL using the Graphene oxide film as SA

CHAPTER 4: RESULT AND DISCUSSION

4.1 Introduction

For developing the SA for generated pulse by Q-switching, various methods and new materials are presented. Rarely transition metal elements from metal nanoparticles-based SA are explored. A really interest amongst scientific researchers is growing up because of these elements. They hold a unique optical property such as large third-order nonlinearity, broad saturable absorption band, and ultrafast response time as discussed in the previous chapters. In the previous chapter, two metal oxides materials; Graphene Oxide (GO) and Carbon nanotube (CNT) were fabricated and characterized. The proposed configuration of the Q-switched ring Erbium-doped fiber laser (EDFL) was also described. This chapter discusses about the result for two Q-switching experiments using the fabricated transition metal oxides saturable absorbers.

4.2 Q-switched EDFL with CNT based SA

At a relatively low threshold pump power (0.054 mW), a stable Q-switched pulse trains were gotten. The pump power is maintained to 28.038 mW to operate passively Q-switching. Fig. 4.1 illustrates the typical optical spectrum at the pump power of 28.038 mW of the Q-switched pulse. It presents a peak pulse of wavelength at 1559.04 nm with a 26.30 dB spectral bandwidth of about 5nm. In the ring cavity, the self-phase modulation effect causes probably the spectral broadening. The typical Q-switching pulse train is presented in figure. 4.2(a) and (b) with a pulse period of 34.2 and 14.8 µs. The pulse repetition rate corresponds to 0.054 kHz and 28.038 kHz, respectively. on the oscilloscope, both pulse trains are stable with no significant pulse jitter seen. At high pump power of 28.038mW, some ripples are observed at the peak of single-pulse profile due to mode beating phenomenon. Pulsing phenomena is observed when CNT-PEO film insert inside the laser cavity. Therefore, we conclude that; the CNT in the EDFL cavity is the main responsible for inducing Q-switching pulse.

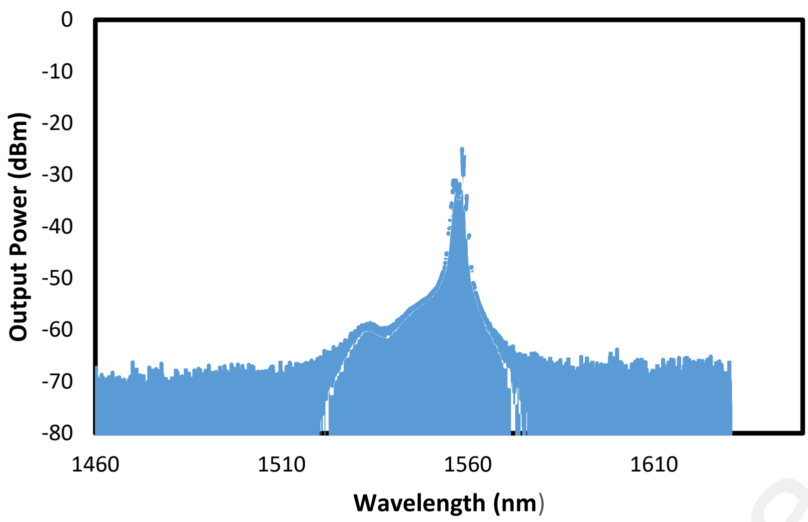

Figure 4.1: Typical optical spectrum of the proposed Q-switched EDFL at pump power of 28.038 Mw

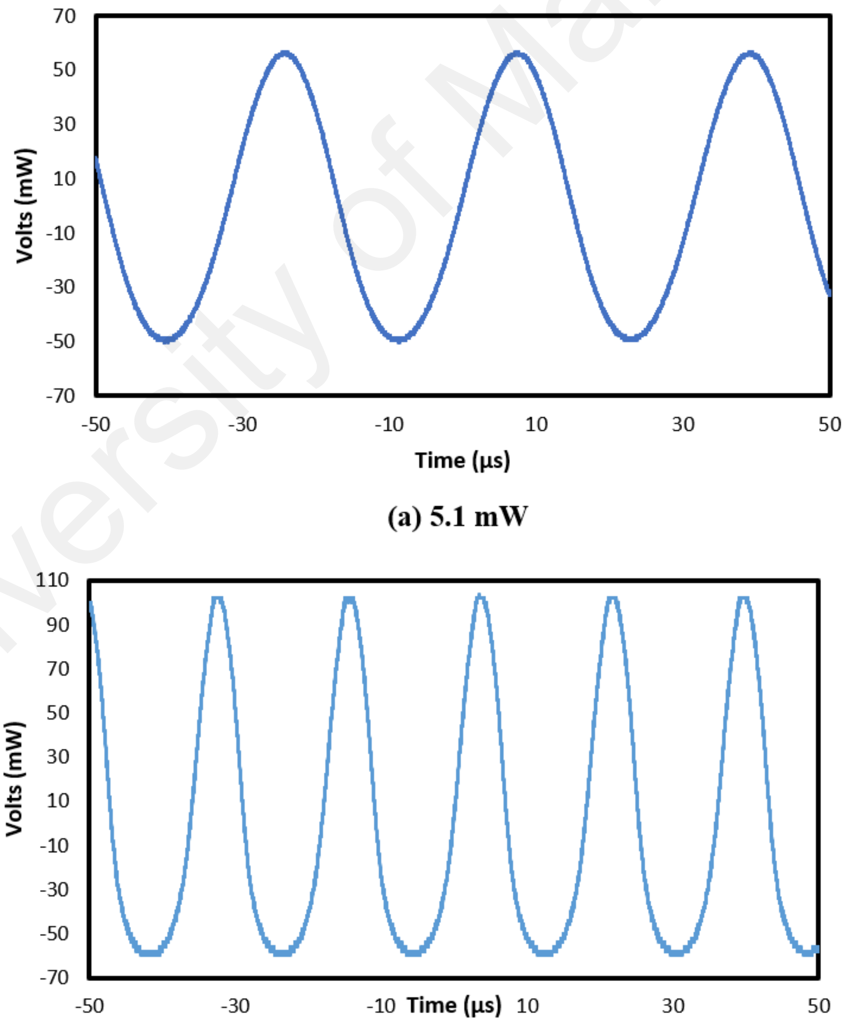

Figure 4.2: Typical typical oscilloscope trace of the proposed Q-switched EDFL at pump power of (a) 0.054 mW and (b) 28.038 mW.

the Q-switched laser performance further investigation is dons to study the characteristics of the output pulses with respect to the incident pump power, for example; the pulse duration, output power, and repetition rate pulse energy. Fig. 4.3 describes the results of incident pump power in terms of pulse repetition rate and pulse width of the laser. From 31.53 to 55.04 kHz, the repetition rate increases nearly monotonously while the pulse width decreased from 14.65 to 6.224 μs as the pump power is boosted from the threshold power of 0.054 to 28.038 mW. These are typical signature of Q-switching operation where the repetition rate and pulse width are pump dependent. The relation between pulse width and repetition rate inversely proportional, that means increasing the pump power causes increasing the repetition rate. As a result, the pulse width decreased. Others Q-switched lasers result is consistent (R. Paschotta, 1999). The SA saturate is provided more gain when increasing the pump power. Hence, the threshold energy stored in the EDF to generate a pulse was reached earlier. As a result, the repetition rate is increasing while the pulse width is reducing.

The Q-switched pulse output was stable with no significant pulse-intensity fluctuation on the oscilloscope as we increase the pump power Moreover, as presented in Fig. 4.4, the calculated single pulse energy corresponds to measure output power of the pulse. The output power superfast from 0.54045 to 2.63 mW on increasing the pump power from 0.054 to 28.038 mW. The pulse energy grew fast. The maximum pulse energy was 47.7834 nJ.

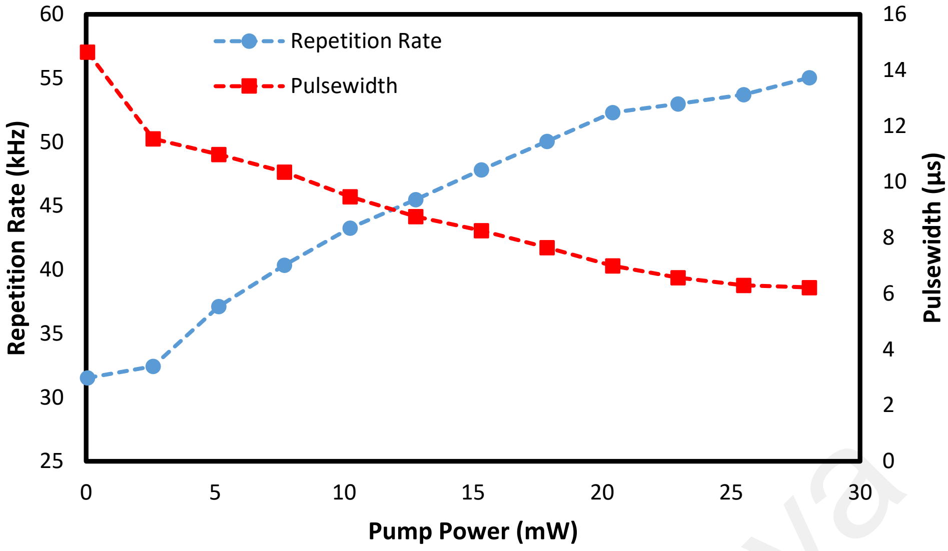

Figure 4.3: Repetition rate and pulse width as functions of input pump power

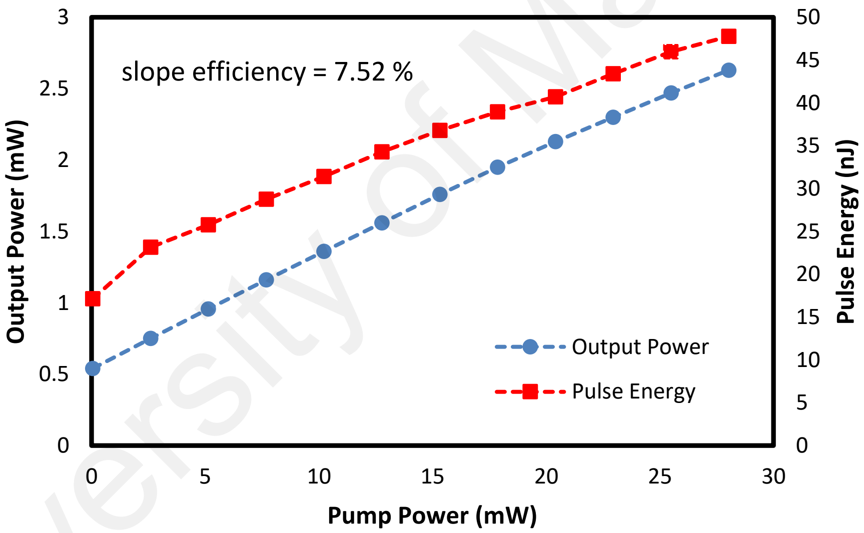

Figure 4.4: Average output power and single-pulse energy as functions of input pump power

The Q-switching operation stability is evaluated by measuring the output spectrum RF of the Q-switch pulses with a span of 189.81 KHz. The pulse repetition rate is 55.04 KHz is indicated from the result is presented in Fig. 4.5. The value of the signal-to-noise ratio (SNR) is more than 74.68 dB, indicating a fair Q-switching stability. The CNT nanoparticles are a potential SA especially at a low pumping strength for Q-switched fiber lasers as appear from the results.

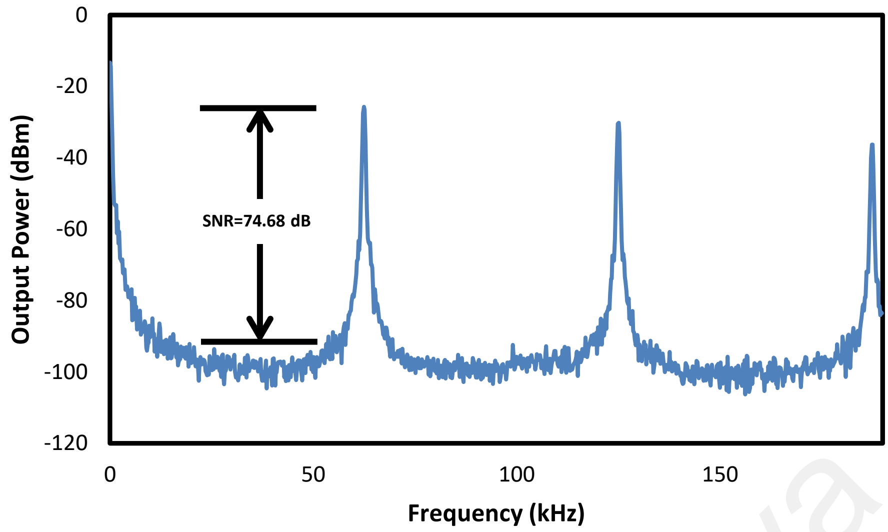

Figure 4.5: RF spectrum at pump power of -2.49mW

4.3 Q-switched EDFL with GO based SA

A stable Q-switched pulse trains are gotten at a relatively low threshold pump power of -2.49 mW. The pump power of 84.006 mW maintained up for Q-switching operation. Fig. 4.1 illustrates the typical optical spectrum of the Q-switched pulse at the pump power of 84.006 mW. It appears a peak wavelength of the pulse at 1558.186 nm with a -22.799 dBm spectral bandwidth of about 5nm. In the ring cavity, the self-phase modulation effect is broadening the spectral. Figs. 4.2(a) and (b) show the typical Q-switching pulse train with a pulse period of 3518.83and 3.855 μs, which corresponds to pulse repetition rate of 22.32 kHz and 72.52 kHz, respectively. Both pulse trains are stable with no significant pulse jitter seen on the oscilloscope. At high pump power of 84.006mW, some ripples are observed at the peak of single-pulse profile due to mode beating phenomenon. Pulsing phenomena is observed when GO-PVA film insert inside the laser cavity. Therefore, we conclude that; the GO in the EDFL cavity is the main responsible for inducing Q-switching pulse.

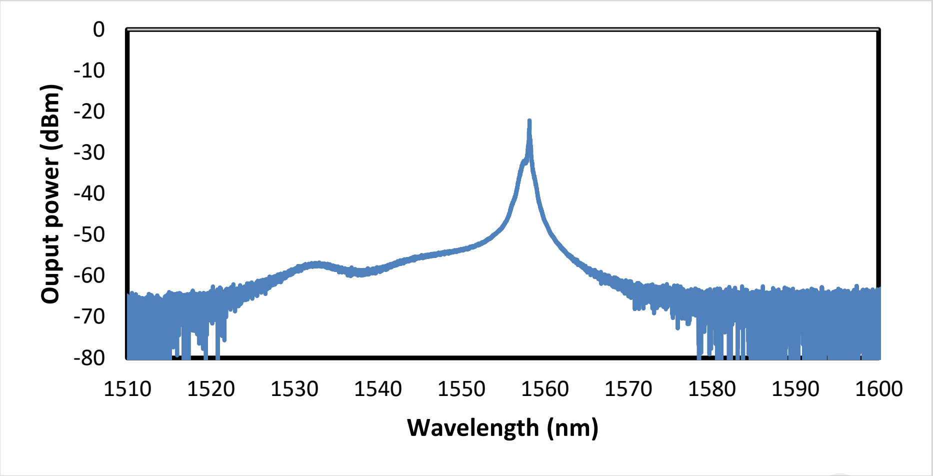

Figure 4.6: Typical optical spectrum of the proposed Q-switched EDFL at pump power of 28.038 Mw

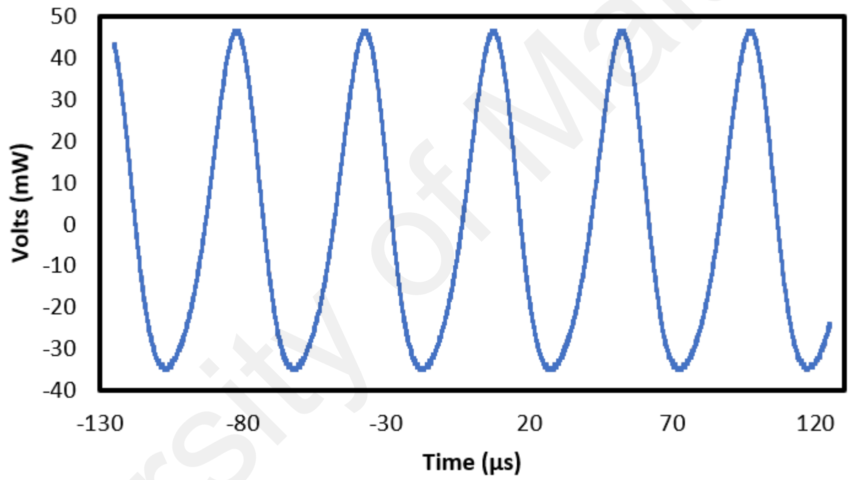

(a) 2.49 mW

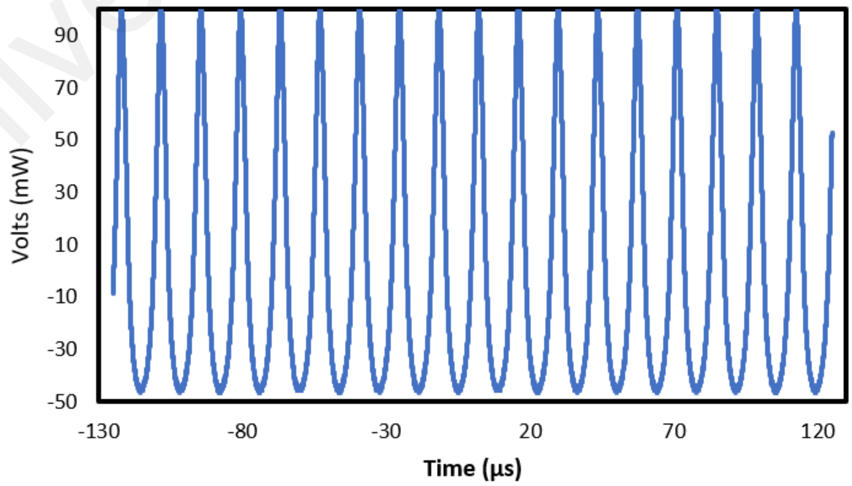

(b) 73.83 mW

Figure 4.7: Typical oscilloscope trace of the proposed Q-switched EDFL at pump power of (a) -2.49 mW and (b) 84.006 mW

the Q-switched laser performance further investigation is dons to study the characteristics of the output pulses with respect to the incident pump power, for example; the pulse duration, output power, and repetition rate pulse energy. Fig. 4.3 describes the results of incident pump power in terms of pulse repetition rate and pulse width of the laser. From 22.32 to 72.52 kHz, the repetition rate increases nearly monotonously while the pulse width decreased from 18.839 to 3.855 μs as the pump power is boosted from the threshold power of-2.49 to 84.006 mW. These are typical signature of Q-switching operation where the repetition rate and pulse width are pump dependent. The relation between pulse width and repetition rate inversely proportional, that means increasing the pump power causes increasing the repetition rate. As a result, the pulse width decreased. Others Q-switched lasers result is consistent (R. Paschotta, 1999). The SA saturate is provided more gain when increasing the pump power. Hence, the threshold energy stored in the EDF to generate a pulse was reached earlier. As a result, the repetition rate is increasing while the pulse width is reducing.

The Q-switched pulse output was stable with no significant pulse-intensity fluctuation on the oscilloscope as we increase the pump power Moreover, as presented in Fig. 4.4, the calculated single pulse energy corresponds to measure output power of the pulse. The output power superfast from 0.54045 to 2.63 mW on increasing the pump power from 0.36272 to 7.16 mW. The pulse energy grew fast. The maximum pulse energy was 98.73 nJ.

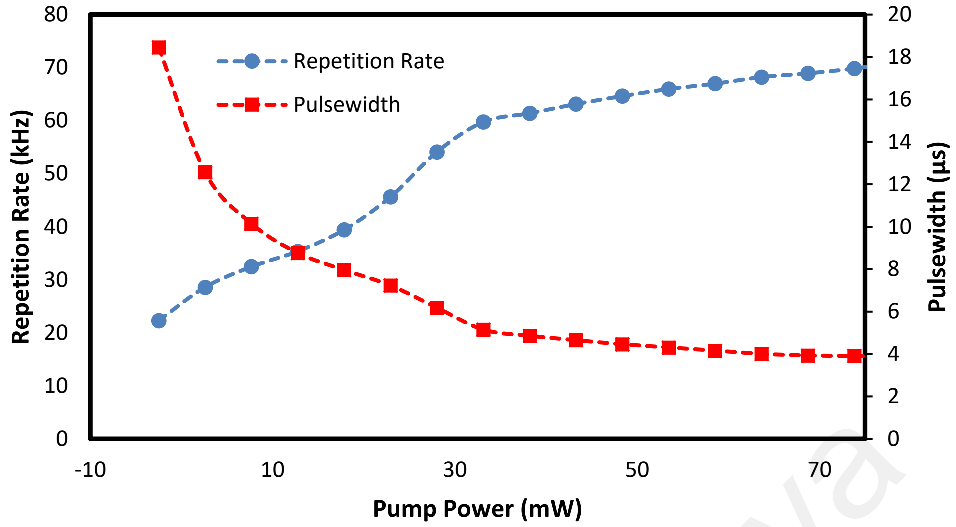

Figure 4.8: Repetition rate and pulse width as functions of input pump power

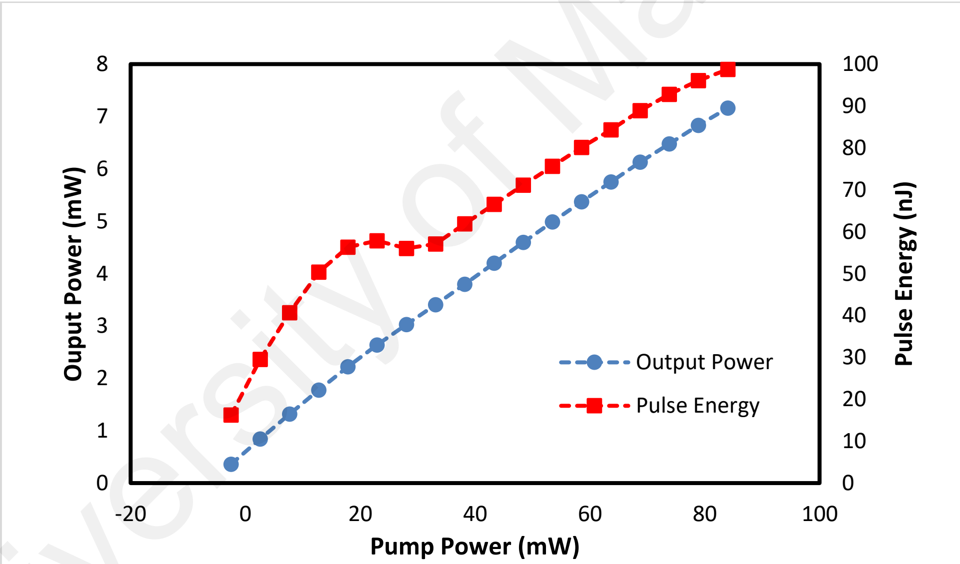

Figure 4.9: Average output power and single-pulse energy as functions of input pump power

The Q-switching operation stability is evaluated by measuring the output spectrum RF of the Q-switch pulses with a span of 356.94 KHz. The pulse repetition rate is 5.35 KHz is indicated from the result is presented in Fig. 4.9.

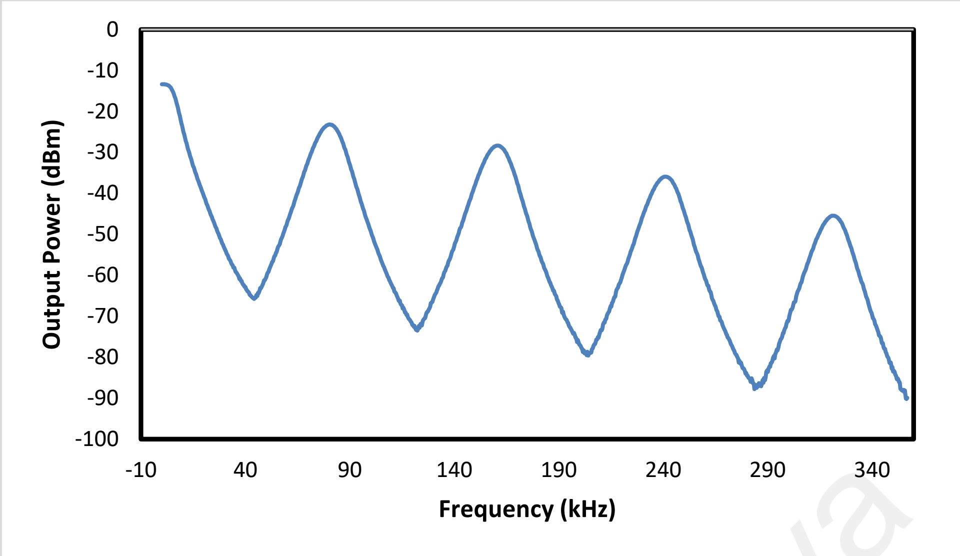

Figure 4.10. RF spectrum at pump power of 200 mW

Table 4.1. CNT vs Go Parameters

CNT	Parameter	GO
0.054 mW to 28.038 mW	Pump Power (mW)	2.49 to 84.006 mW
0.5454 mW to 2.63mW	Output Power (mW)	0.36272 mW to 7.16 mW
31.53 kHz to 55.04 kHz	Rr (kHz)	22.32 kHz to 72.52 kHz
14.65 µs to 6.22µs	Pulse Width (µs)	18.839 µs to 3.855 µs
47.7834 nJ	Pulse Energy (nJ)	98.73 nJ

CHAPTER 5: CONCLUSION

The research work aimed to demonstrate Q-switched Erbium-doped fiber lasers (EDFLs) utilizing transition metal oxide based saturable absorber (SA). Two types of SAs were explored in this study; graphene oxide (GO) and carbon nanotube (CNT). At first, the CNT based SA was successfully fabricated based on CNT nanoparticles in conjunction with polyethylene oxide (PEO) polymer. The preparation and characterization of the SA was described in Chapter 3. CNT nanoparticles were synthesized by facile nonchemical method because it does not require any surfactants and complex process. The produced CNT SA was characterized by FESEM. CNT film was obtained by incorporating a GO nanoparticle into a polyvinyl alcohol

(PVA). A piece of 1 mm x 1 mm the metal oxide film was sandwiched in between two fiber ferrules via a fiber connector and incorporated into the Erbium-doped fiber laser (EDFL) cavity for Q-switching pulse generation experiments. At first, the Q-switched EDFL was demonstrated in using a CNT/PEO film as SA. The laser was self-started and generate stable pulse train by changing the pump power from 0 mW to 28.038 mW with repetition rate that can be widely tuned from 0.054 kHz and 28.038 kHz. It operates at 1559.04 nm wavelength and the output power increases from 1.18 to 6.57 mW as the pump power is increased from the threshold power of 0 mW to 28.038 mW. The Q-switched pulse train has a pulse width 14 µs and the pulse energy 47.7834 nJ, at the maximum pump power 28.038 mW. The RF spectrum showed the signal noise to ratio of more than 74.86 dB, which indicates the stability of the Q-switching operation. The repetition rate is much lower and the pulse width is wider compared the passive mode locked technique.

In another experiment, passively Q-switched EDFL was also demonstrated using GO embedded into PVA film as a SA. By inserting the SA into an EDFL ring cavity, stable

Q-switching pulse operating at 1558.186 nm was obtained at threshold pump power f - 2.49 mW, smaller than the previous CNT based EDFL. The repetition rate of the laser varies from 22.32 kHz and 69.83 kHz as the 980-nm pump power increased from -2.49 mW to 73.83 mW. The Q-switching operating has the shortest pulse width of 5.44 µs, and the maximum pulse energy up to 98.73 nJ. The Q-switching pulse shows no spectral modulation with a peak-to-pedestal ratio of 90 dB indicating the high stability of the laser.

Based on these results, it is found that GO film performed better than CNT one in terms of lower threshold pump power and better stability. The experimental results also verify that both GO and CNT films possess the potential advantage for stable Q-switched pulse generation at 1.5 µm

There are several aspects that need to be considerate for further improvements. First, would be by further extending the lengths of EDF gain medium. It would broaden the spectral wavelength and the output power could be increase by changing the length of EDF. Moreover, it will increase the repetition rate as the repetition rate is proportional to the length of the laser cavity. As the repetition rate is inversely proportional to the pulse width, the pulse width will be decreased as the repetition rate increases. In addition, in order to reduce the losses in the cavity, we can minimize the employment of pigtails. This is because the losses in the pigtails fiber tip can give high nonlinearity in the laser ring cavity. Future studies should be focusing on exploring more on the optical properties of both GO and CNT SA for ultrafast laser generation.

REFERENCES

Ahmad, H., Ismail, M. A., Suthaskumar, M., Tiu, Z. C., Harun, S. W., Zulkifli, M. Z., . . . Sivaraj, S. (2016). S-band Q-switched fiber laser using molybdenum disulfide (MoS2) saturable absorber. *Laser Physics Letters, 13*(3), 035103.

Ahmad, H., Lee, C., Ismail, M., Ali, Z., Reduan, S., Ruslan, N., . . . Harun, S. (2016). Zinc oxide (ZnO) nanoparticles as saturable absorber in passively Q-switched fiber laser. *Optics Communications, 381*, 72-76.

Ahmad, H., Reduan, S. A., Ali, Z. A., Ismail, M., Ruslan, N., Lee, C., . . . Harun, S. (2016). C-band Q-switched fiber laser using titanium dioxide (TiO 2) as saturable absorber. *IEEE Photonics Journal, 8*(1), 1-7.

Ahmad, H., Ruslan, N., Ismail, M., Ali, Z., Reduan, S., Lee, C., & Harun, S. (2016). Silver nanoparticle-film based saturable absorber for passively Q-switched erbium-doped fiber laser (EDFL) in ring cavity configuration. *Laser Physics, 26*(9), 095103.

Ahmad, H., Ruslan, N., Ismail, M., Reduan, S., Lee, C., Sathiyan, S., . . . Harun, S. (2016). Passively Q-switched erbium-doped fiber laser at C-band region based on WS 2 saturable absorber. *Applied optics, 55*(5), 1001-1005.

Ahmad, H., Soltanian, M., Narimani, L., Amiri, I., Khodaei, A., & Harun, S. (2015). Tunable S-band Q-switched fiber laser using Bi 2 Se 3 as the saturable absorber. *IEEE Photonics Journal, 7*(3), 1-8.

Ahmad, H., Thambiratnam, K., Muhammad, F. D., Zulkifli, M. Z., Zulkifli, A. Z., Paul, M. C., & Harun, S. W. (2014). Q-Switching and Mode-Locking in Highly Doped Zr $ _ {2} $ O $ _ {3} $–Al $ _ {2} $ O $ _ {3} $–Er $ _ {2} $ O $ _ {3} $-Doped Fiber Lasers Using Graphene as a Saturable Absorber. *IEEE Journal of Selected Topics in Quantum Electronics, 20*(1), 9-16.

Anyi, C., Ali, N., Rahman, A., Harun, S., & Arof, H. (2013). Multi-wavelength Q-switched erbium-doped fibre laser using saturable absorber based on carbon nanotube film. *Ukrainian journal of physical optics*(14,№ 4), 212-218.

Bai, X., Mou, C., Xu, L., Wang, S., Pu, S., & Zeng, X. (2016). Passively Q-switched erbium-doped fiber laser using Fe3O4-nanoparticle saturable absorber. *Applied Physics Express, 9*(4), 042701.

Bao, Q., Zhang, H., Wang, Y., Ni, Z., Yan, Y., Shen, Z. X., . . . Tang, D. Y. (2009). Atomic-layer graphene as a saturable absorber for ultrafast pulsed lasers. *Advanced Functional Materials, 19*(19), 3077-3083.

Chang, Y. M., Kim, H., Lee, J. H., & Song, Y.-W. (2010). Multilayered graphene efficiently formed by mechanical exfoliation for nonlinear saturable absorbers in fiber mode-locked lasers. *Applied Physics Letters, 97*(21), 211102.

Chang, Y. M., Kim, H., Lee, J. H., & Song, Y.-W. (2011). *Passive mode-locker incorporating physically exfoliated graphene for fiber ring lasers.* Paper presented at the Optical Fiber Communication Conference and Exposition (OFC/NFOEC), 2011 and the National Fiber Optic Engineers Conference.

Choudhary, A., Dhingra, S., D'Urso, B., Kannan, P., & Shepherd, D. P. (2015). Graphene Q-switched mode-locked and Q-switched ion-exchanged waveguide lasers. *IEEE Photonics Technol. Lett., 27*(6), 646-649.

Fermann, M. E., & Hartl, I. (2013). Ultrafast fibre lasers. *Nature photonics, 7*(11), 868.

Hasan, T., Sun, Z., Wang, F., Bonaccorso, F., Tan, P. H., Rozhin, A. G., & Ferrari, A. C. (2009). Nanotube–polymer composites for ultrafast photonics. *Advanced Materials, 21*(38-39), 3874-3899.

Hisamuddin, N., Zakaria, U., Zulkifli, M., Latiff, A., Ahmad, H., & Harun, S. (2016). Q-Switched Raman Fiber Laser with Molybdenum Disulfide-Based Passive Saturable Absorber. *Chinese Physics Letters, 33*(7), 074208.

Ismail, E., Kadir, A., Latiff, A., Ahmad, H., & Harun, S. (2016). Q-switched erbium-doped fiber laser operating at 1502 nm with molybdenum disulfide saturable absorber. *Journal of Nonlinear Optical Physics & Materials, 25*(02), 1650025.

Ismail, E., Kadir, N., Latiff, A., Ahmad, H., & Harun, S. (2016). Black phosphorus crystal as a saturable absorber for both a Q-switched and mode-locked erbium-doped fiber laser. *RSC Advances, 6*(76), 72692-72697.

Ismail, M., Ahmad, F., Harun, S., Arof, H., & Ahmad, H. (2013). A Q-switched erbium-doped fiber laser with a graphene saturable absorber. *Laser Physics Letters, 10*(2), 025102.

Ismail, M. A., Harun, S. W., Ahmad, H., & Paul, M. C. (2016). Passive Q-switched and Mode-locked Fiber Lasers Using Carbon-based Saturable Absorbers *Fiber Laser*: InTech.

Jauregui, C., Limpert, J., & Tünnermann, A. (2013). High-power fibre lasers. *Nature photonics, 7*(11), 861.

Ji, H., Oxenløwe, L. K., Galili, M., Rottwitt, K., Jeppesen, P., & Grüner-Nielsen, L. (2008). *Fiber optical trap deposition of carbon nanotubes on fiber end-faces in a modelocked laser*. Paper presented at the Conference on Lasers and Electro-Optics.

Jiang, K., Wu, Z., Fu, S., Song, J., Li, H., Tang, M., . . . Liu, D. (2016). Switchable dual-wavelength mode-locking of thulium-doped fiber laser based on SWNTs. *IEEE Photonics Technology Letters, 28*(19), 2019-2022.

Kashiwagi, K., & Yamashita, S. (2009). Deposition of carbon nanotubes around microfiber via evanascent light. *Optics express, 17*(20), 18364-18370.

Kashiwagi, K., Yamashita, S., & Set, S. Y. (2009). In-situ monitoring of optical deposition of carbon nanotubes onto fiber end. *Optics express, 17*(7), 5711-5715.

Kasim, N., Al-Masoodi, A., Ahmad, F., Munajat, Y., Ahmad, H., & Harun, S. (2014). Q-switched ytterbium doped fiber laser using multi-walled carbon nanotubes saturable absorber. *Chinese optics letters, 12*(3), 031403.

Kelleher, E., Travers, J., Sun, Z., Rozhin, A., Ferrari, A., Popov, S., & Taylor, J. (2009). Nanosecond-pulse fiber lasers mode-locked with nanotubes. *Applied Physics Letters, 95*(11), 111108.

Lamhot, Y., Barak, A., Peleg, O., & Segev, M. (2010). Self-trapping of optical beams through thermophoresis. *Physical review letters, 105*(16), 163906.

Li, H., Xia, H., Lan, C., Li, C., Zhang, X., Li, J., & Liu, Y. (2015). Passively $ Q $-switched erbium-doped fiber laser based on few-layer MoS 2 saturable absorber. *IEEE Photonics Technology Letters, 27*(1), 69-72.

Lin, Y.-H., Yang, C.-Y., Liou, J.-H., Yu, C.-P., & Lin, G.-R. (2013). Using graphene nano-particle embedded in photonic crystal fiber for evanescent wave mode-locking of fiber laser. *Optics express, 21*(14), 16763-16776.

Luo, A., Luo, Z., Xu, W., Dvoyrin, V., Mashinsky, V., & Dianov, E. (2011). Tunable and switchable dual-wavelength passively mode-locked Bi-doped all-fiber ring laser based on nonlinear polarization rotation. *Laser Physics Letters, 8*(8), 601.

Maiman, T. H. (1960). Stimulated optical radiation in ruby.

Marowsky, G. (1976). Principles of dye laser operation and dye laser tuning methods. *Optica Acta: International Journal of Optics, 23*(11), 855-872.

Martinez, A., Fuse, K., Xu, B., & Yamashita, S. (2010). Optical deposition of graphene and carbon nanotubes in a fiber ferrule for passive mode-locked lasing. *Optics express, 18*(22), 23054-23061.

Martinez, A., Fuse, K., & Yamashita, S. (2011). Mechanical exfoliation of graphene for the passive mode-locking of fiber lasers. *Applied Physics Letters, 99*(12), 121107.

Méndez, A., & Morse, T. F. (2011). *Specialty optical fibers handbook*: Elsevier.

Nicholson, J., Windeler, R., & DiGiovanni, D. (2007). Optically driven deposition of single-walled carbon-nanotube saturable absorbers on optical fiber end-faces. *Optics express, 15*(15), 9176-9183.

Okhotnikov, O., Kuzmin, V., & Salcedo, J. (1994). General intracavity method for laser transition characterization by relaxation oscillations spectral analysis. *IEEE Photonics Technology Letters, 6*(3), 362-364.

Paschotta, D. R. R. P. E. S. A.

Paschotta, R. (2008). *Encyclopedia of laser physics and technology* (Vol. 1): Wiley-vch Berlin.

Paschotta, R., Häring, R., Gini, E., Melchior, H., Keller, U., Offerhaus, H., & Richardson, D. (1999). Passively Q-switched 0.1-mJ fiber laser system at 1.53? m. *Optics letters, 24*(6), 388-390.

Pérez-Millán, P., Cruz, J., & Andrés, M. (2005). Active Q-switched distributed feedback erbium-doped fiber lasers. *Applied Physics Letters, 87*(1), 011104.

Popa, D., Sun, Z., Hasan, T., Torrisi, F., Wang, F., & Ferrari, A. (2011). Graphene Q-switched, tunable fiber laser. *Applied Physics Letters, 98*(7), 073106.

Set, S. Y., Yaguchi, H., Tanaka, Y., Jablonski, M., Sakakibara, Y., Rozhin, A., . . . Kikuchi, K. (2003). *Mode-locked fiber lasers based on a saturable absorber incorporating carbon nanotubes.* Paper presented at the Optical Fiber Communication Conference.

Singh, S. C., Zeng, H., Guo, C., & Cai, W. (2012). *Nanomaterials: processing and characterization with lasers*: John Wiley & Sons.

Siniaeva, M., Siniavsky, M., Pashinin, V., Mamedov, A. A., Konov, V., & Kononenko, V. (2009). Laser ablation of dental materials using a microsecond Nd: YAG laser. *Laser Physics, 19*(5), 1056-1060.

Sobon, G. (2016). Application of 2D Materials to Ultrashort Laser Pulse Generation *Two-dimensional Materials-Synthesis, Characterization and Potential Applications*: InTech.

Song, Y.-W., Yamashita, S., Goh, C. S., & Set, S. Y. (2007). Carbon nanotube mode lockers with enhanced nonlinearity via evanescent field interaction in D-shaped fibers. *Optics letters, 32*(2), 148-150.

Sun, Z., Hasan, T., Torrisi, F., Popa, D., Privitera, G., Wang, F., . . . Ferrari, A. C. (2010). Graphene mode-locked ultrafast laser. *ACS nano, 4*(2), 803-810.

Wang, F., Torrisi, F., Jiang, Z., Popa, D., Hasan, T., Sun, Z., . . . Ferrari, A. C. (2012). *Graphene passively Q-switched two-micron fiber lasers.* Paper presented at the Lasers and Electro-Optics (CLEO), 2012 Conference on.

Wang, J., Yang, P., Wei, X., & Zhou, Z. (2015). Preparation of NiO two-dimensional grainy films and their high-performance gas sensors for ammonia detection. *Nanoscale research letters, 10*(1), 119.

Woodward, R., Kelleher, E., Howe, R., Hu, G., Torrisi, F., Hasan, T., . . . Taylor, J. (2014). Tunable Q-switched fiber laser based on saturable edge-state absorption in few-layer molybdenum disulfide (MoS 2). *Optics express, 22*(25), 31113-31122.

Yamashita, S. (2012). A tutorial on nonlinear photonic applications of carbon nanotube and graphene. *Journal of lightwave technology, 30*(4), 427-447.

Yamashita, S., Inoue, Y., Maruyama, S., Murakami, Y., Yaguchi, H., Jablonski, M., & Set, S. (2004). Saturable absorbers incorporating carbon nanotubes directly synthesized onto substrates and fibers and their application to mode-locked fiber lasers. *Optics letters*, *29*(14), 1581-1583.

Yamashita, S., Set, S. Y., Goh, C. S., & Kikuchi, K. (2007). Ultrafast saturable absorbers based on carbon nanotubes and their applications to passively mode-locked fiber lasers. *Electronics and Communications in Japan (Part II: Electronics)*, *90*(2), 17-24.

Zhao, J., Ruan, S., Yan, P., Zhang, H., Yu, Y., Wei, H., & Luo, J. (2013). Cladding-filled graphene in a photonic crystal fiber as a saturable absorber and its first application for ultrafast all-fiber laser. *Optical Engineering*, *52*(10), 106105.